26 May 2010, 4:45 pm - 6:45 pm

Effect of Elastic and Inelastic DSSI on Seismic Demands of SDOFs Structures

Esteban Sáez
Pontificia Universidad Católica de Chile, Chile

Fernando López-Caballero
École Centrale Paris, France

Arézou Modaressi-Farahmand-Razavi
École Centrale Paris, France


Fifth International Conference on
Recent Advances in Geotechnical Earthquake Engineering and Soil Dynamics
and Symposium in Honor of Professor I.M. Idriss
May 24-29, 2010 • San Diego, California

EFFECT OF ELASTIC AND INELASTIC DSSI ON SEISMIC DEMANDS OF SDOFS STRUCTURES

Esteban Sáez

Lab. MSSMAT CNRS UMR 8579, Ecole Centrale Paris
Châtenay-Malabry, France
Current Position: Departement of Structural and Geotechnical Engineering, Pontificia Universidad Católica de Chile, Santiago, Chile

Fernando López-Caballero
Arézou Modaressi-Farahmand-Razavi
Lab. MSSMAT CNRS UMR 8579, Ecole Centrale Paris
Châtenay-Malabry, France

ABSTRACT

In general, under earthquake loading, the soil reaches the limit of its elastic behavior before the structural elements. Thus, an earthquake analysis approach assuming inelastic structural behavior under fixed base condition or with elastic dynamic soil-structure interaction (DSSI) hypothesis may be inadapted. This paper describes the investigation conducted in order to define the contribution of the pure elastic DSSI effects in the complete inelastic DSSI problem. With this purpose, a comparative analysis between elastic and inelastic soil behavior assumptions for two inelastic single-degree-of-freedom (SDOF) structures and two soils is carried out. The results point out that, in general, inelastic soil behavior plays a decisive role only when the soil is saturated. When the soil is in dry condition, an elastic DSSI approach seems to be accurate enough to take into account the modification of the structural response due to DSSI. Differences in structural dynamics responses are related to pore pressure generation induced in the inelastic case and neglected when elastic soil behavior is assumed.

INTRODUCTION

The influence of the interaction of the soil with a superstructure on its dynamic behavior has been the subject of numerous investigations assuming linearity of both, superstructure and soil foundation. For elastic systems, first studies for soil-structure interacting systems were conducted by Jennings and Bielak (1973); Veletsos and Meek (1974); Veletsos and Nair (1975) for surface-supported structures. In these works, the effects of the inertial DSSI are summarized by an equivalent SDOF characterizing support ground flexibility and the foundation damping. The effect of the flexible soil is included by modifying the fixed base fundamental period. The foundation damping associated to radiation and soil material damping is introduced by defining an effective damping of the superstructure-foundation system as the sum of a term proportional to viscous damping in the structure plus an equivalent viscous foundation damping. The increase of the natural period and the added foundation damping have been extensively studied by several authors (e.g., Veletsos (1977); Luco (1980); Wolf (1985); Avilés and Pérez-Rocha (1996)). Nevertheless, this replacement oscillator approach is strictly valid only for elastic superstructure-foundation systems. This aspect is a significant limitation for earthquake engineering, where inelastic superstructure behavior is intentionally accepted. Despite the elastic intrinsic assumption, this approach has been included in several seismic design provisions (e.g. ATC 40, FEMA 356, FEMA 450), using free-field response spectra combined with effective values of both, fundamental period and equivalent viscous damping including elastic DSSI.

In principle, the effect of DSSI may differ between elastic and inelastic systems. Thus, the current interaction provisions based on elastic response studies could not be directly applicable to seismic design of typical buildings, expected to deform considerably beyond the yield limit during severe earthquakes (Avilés and Pérez-Rocha, 2003). According with the works of Veletsos (1977), the yielding of the superstructure can be viewed as a general increase of the

relative flexibility between the superstructure and the soil, resulting into a reduction of DSSI effects. Unfortunately, the effects of the DSSI on yielding superstructure systems have not been extensively studied. Theoretical studies conducted by Priestley (1987) for elastoplastic bridge piers showed that the foundation compliance reduces the ductility capacity of the system. More recently, several other studies using the replacement oscillator technique Ciampoli and Pinto (1995); Rodriguez and Montes (2000); Gazetas and Mylonakis (2001); Avilés and Pérez-Rocha (2003), have been conducted in order to elucidate the effect of the DSSI on the maximum required ductility. Similarly, Ghannad and Jahankhah (2007) use the replacement oscillator method to study the effect of DSSI on strength reduction factors of elastoplastic SDOFs. These studies point out some configurations were the DSSI has a considerable effect on the ductility demand of structures.

In the studies listed above, the soil replacement spring and dashpots are selected using frequency-independent approximations of the solutions available for dynamic impedances of rigid footings on elastic soil profiles, using Cone models, or using series of linear springs and dashpots attached to the base foundation. Despite the used method, the numerical values of the soil replacement spring and dashpot are dependent on the shear wave velocity. As shear wave velocity decreases when the soil shear strain increases, some of these authors use degraded shear wave velocity values in their models. Experimental results show that the limit of linear-elastic soil behavior is very low ($\gamma<10^{-5}$). This shear strain limit is normally exceeded during motions inducing damage of superstructures. Nevertheless, as described in Sáez (2009), superstructure's self weight increases the soil confinement under the foundation reducing locally the energy dissipation by hysteresis. Indeed, larger soil energy dissipation takes place in less confined zones. Consequently, the solely modification of the shear wave velocity under the foundation does not seem an appropriate approach to take into account the contribution of the inelastic soil behavior. Results presented in author's previous work highlight the effect of the combined DSSI effects and non-linear soil behavior on the computed structural response. Nevertheless, the separation of the contribution of each phenomenon to the total response is not easy to identify due to the complexity of the problem. This paper describes the investigation conducted in order to compare the contribution of elastic and inelastic DSSI effects on the inelastic seismic response of structures.

METHODS OF ANALYSIS

In order to evaluate the contribution of the DSSI in the modification of the structures' dynamic response, two kinds of dynamic time-domain analyses are conducted:

- Non-linear dynamic fixed base superstructure computations using as input motion the free field acceleration obtained for elastic (TS-E) and non-linear (TS-N) soil columns.
- Complete dynamic soil-foundation-superstructure FE analyses, considering elastic (SSI-E) and non-linear (SSI-N) soil behavior.

The two approaches are presented schematically in Fig. 1. This comparative approach was developed in order to provide two groups of consistent responses. The simple comparison of the SSI-E or SSI-N approaches with the fixed base response imposing outcropping bedrock input motion is not adequate, because site effects will be neglected. TS-E or TS-N approaches corresponds to the state of the practice in earthquake engineering. In this work, wave propagation part of the TS-N approach is achieved using an elastoplastic soil constitutive model (Aubry *et al.*, 1982; Hujeux, 1985). However, this step can be performed through the widely used equivalent-liner approach (Schnabel *et al.*, 1972), or by employing 1D constitutive models (Lopez-Caballero et al., 2007) among others. The computed free field response can be injected later as input for any commercial non-linear structural dynamic code. On the contrary, a complete non-linear dynamic soil-structure interaction is still out of the today's engineering practice.

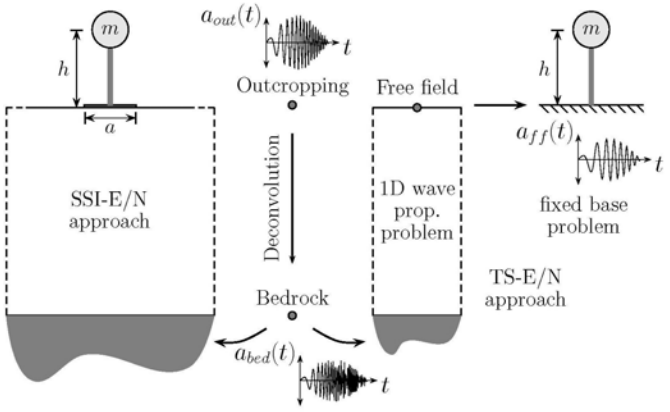

Fig. 1. Proposed approaches: complete SSI model v/s two-step computation.

Both, TS-N and TS-E cases take into account inelastic structural behavior but neglect DSSI effects. Complete DSSI analyses, SSI-E or SSI-N, include dynamic interaction effects and superstructure material non-linearities. Details regarding each model, assumptions and parameters are provided in the following. The simulations were performed with the Finite Element code *GEFDyn* (Aubry *et al.*, 1986; Aubry and Modaressi, 1996).

Superstructure modeling

The superstructures considered in this paper are modeled by a massless continuous column of height *h* with a single mass *m* on top. The foundation is assumed square of side *a* (Fig.1). These superstructures respond as a SDOF system with a

fundamental period T_0 in fixed-base condition. Damping is assumed to be hysteretic, controlled by the non-linear constitutive model of the column. Numerical values of properties characterizing each SDOF are selected on the basis of the classification of building types used in HAZUS (2003).

According to this document, reinforced concrete moment frame buildings can be classified as low-rise, mid-rise and high-rise, in terms of the total height and/or the number of stories. In this paper, only C1L (low-rise) and C1M (mid-rise) categories are explored. In order to define the geometric parameters describing the SDOFs, we start assuming a height. The typical height suggested in HAZUS (2003) is selected as height of the equivalent SDOF, i.e. *6* and *15*[m], for low-rise and mid-rise structures, respectively. The choice of the foundation dimension *a* is based on the slender ratio *h/a*. As usually the slender ratio increase with the number of stories of a building, we select slender ratios of *1* and *1.5* for C1L and C1M categories, respectively. The total weight/mass is defined assuming a number of levels and a uniform weight distribution of *10*[kN/m^3] over each level. Assuming *3* and *5* levels, we obtain a total weight of *1080* and *5000*[kN] for C1L and C1M, respectively.

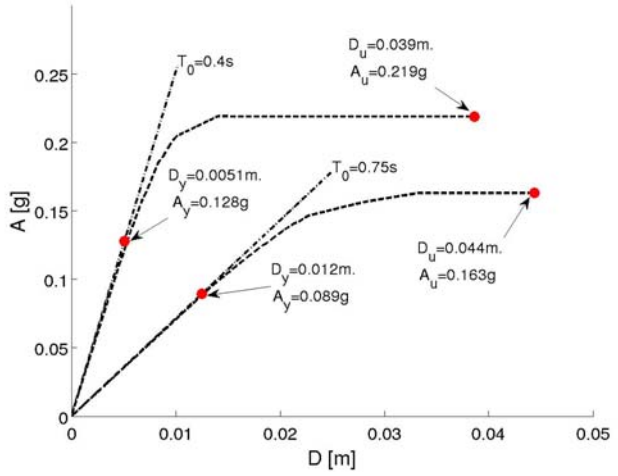

Fig. 2. Computed capacity curves for C1L and C1M SDOFs.

In the HAZUS methodology, some reference parameters are given to develop capacity curves. The value of these parameters depends on the conformity of the studied building to modern seismic design provisions. In this way, four levels are defined: High-Code, Moderate-Code, Low-Code and Pre-Code. The provided value of fixed base fundamental period is fixed as the target value for T_0. The stiffness of the cantilever column of the SDOF model is computed using the value of T_0 and *m*, assuming a constant square transversal section and a fixed value of the Young modulus. To model the post-yielding behavior, we use the Prandtl-Reuss constitutive model. Thus, the values of the hardening modulus and initial yield stress are selected in order to obtain a capacity curve compatible with the ranges defined in HAZUS. The obtained capacity curves are shown in Fig.2. It can be noticed that a maximum ductility μ of *7.6* and *3.7* are computed for C1L and C1M, respectively. These values satisfy the ranges provided in HAZUS and correspond approximately to a Moderate-Code conformity.

Soil profiles' description

In this paper, we consider a dry and a saturated homogenous dense Toyoura sand profiles of *30*[m] depth, overlying an elastic bedrock. The effect of the stiffness increasing with depth is shown in Fig.3 in terms of free field low-strain shear velocity profile. Indeed, the superstructure's self weight increases locally the confinement below the foundation. This additional confinement increases the low-strain shear wave velocity for both, dry and saturated cases. These profiles were computed at the center of the foundation in the DSSI analyses using FE models described below.

According to Fig.3, the influence of the superstructure on the low-strain shear wave velocity reaches approximately *7* and *15*[m] depth, for C1L and C1M structures, respectively. Indeed, in the saturated case, as the initial effective stresses are reduced due to the water table, the over stress imposed by the superstructure has a relatively larger influence on the effective confinement and consequently on the soil stiffness. The computed values of the average shear wave velocity in the upper *30*[m] ($V_{s,30}$) are shown in Fig.3 for each soil. The elastic first periods of the soils (T_{soil}) are *0.46*[s] and *0.54*[s], for dry and saturated cases, respectively.

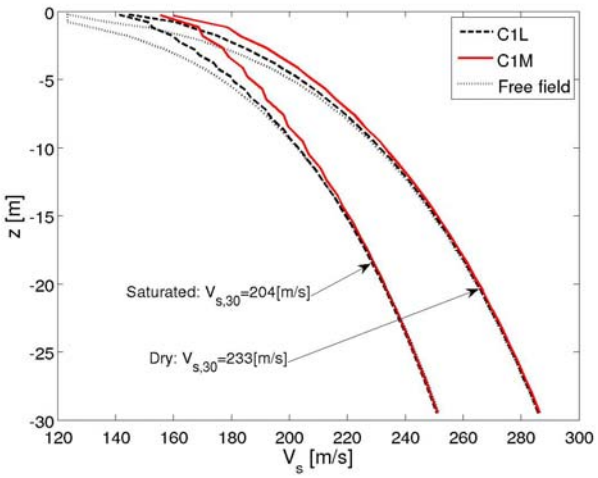

Fig. 3. Low-strain shear wave velocity profiles of studied medium dense sand profile under dry and fully saturated conditions. Influence of superstructure's self weight.

As described above, two kind of constitutive models were used for describing the soil's dynamic behavior: a non-linear elastic model and an elasto-plastic one (Aubry *et al.*, 1982; Hujeux, 1985). In both constitutive models, the influence of the soil confinement is taken into account by a non-linear approach governed by the expressions:

$$K = K_{ref}\left(\frac{p'}{p'_{ref}}\right)^{n_e} \quad (1)$$

$$G = G_{ref}\left(\frac{p'}{p'_{ref}}\right)^{n_e} \quad (2)$$

in terms of reference elastic modulus (K_{ref} and G_{ref}), the mean effective compressive stress p' and the coefficient n_e defining the degree of non-linearity. As identical values of elastic parameters and n_e coefficient have been used for both constitutive models, the low-strain shear wave profiles shown in Fig.3 are valid for both cases. The parameters describing elasto-plastic constitutive model have been calibrated by simulating laboratory soil test (Sáez, 2009) for both dry and saturated condition, using the methodology described in Lopez-Caballero *et al.* (2007). Variations of initial critical pressure p_{c0} and hardening variables due to *in-situ* densities are neglected, thus a homogenous soil profile obeying the same set of parameters is assumed. In saturated condition, a porosity $n=0.54$ and an isotropic permeability of $k = 10^{-4}$[m/s] are supposed.

Fixed base two-step analyses: TS-E and TS-N

The approach consists in solving firstly the shear wave propagation problem for a soil column model obeying the same constitutive model as the full 3D computations. In this case, the corresponding FE model is composed of 3D solid elements using the same vertical discretization as the one used for complete 3D DSSI models. The computed free field motion is imposed afterward as input accelerogram to fixed base models described above. This approach takes into account inelastic behavior of the soil (TS-N) and the superstructure (TS-E and TS-N), but neglects dynamical interaction effects. As the wave propagation part of the problem is solved in free field condition, variations of the low-strain shear wave profile due to over stress imposed by the weight of the superstructure are not considered.

Complete DSSI models: SSI-E and SSI-N

The complete DSSI models are composed of the superstructure, the foundation, the soil and a part of the underlying bedrock. Due to nature of the problem, we use 3D meshes in this case. Consequently, the required time of run in this 3D case increases drastically compared to a standard plane-strain approach. Indeed, plane strain approach requires periodicity across an axis normal to dynamic loading and a rigid foundation. This requirement is not satisfied for a general SDOF model on a finite foundation. This assumption of periodicity was implicitly used in computations presented in previous works (Sáez *et al.*, 2008). In Sáez *et al.* (2009), we introduced a modified 2D in-plane approach allowing to carry out faster analyses of the inelastic DSSI effects on regular buildings. In the study presented in this paper, we relax this hypothesis analyzing the more general 3D case.

The *30*[m] deep homogenous soil deposits considered are modeled by *8* nodes 3D solid elements with displacements and pressure (in saturated case) DOFs. The foundation is supposed to be rigid and modeled also by *8* node 3D volume elements with very stiff mechanical properties. In saturated condition, the ground water level is assumed to be at surface ($z=0$[m]). The so-called *u-p* formulation is used in this case (Zienkiewicz and Shiomi, 1984). We assume impervious condition for both foundation and bedrock. At the bottom of the mesh, paraxial elements (Modaressi and Benzenati, 1994) are used to impose the incident motion and ensure damping by radiation. Lateral limits of the mesh are considered to be far enough from the structure so that periodic condition are verified on them. Consequently, tied condition (Zienkiewicz *et al.*, 1988) have been imposed on the lateral limits of the meshes. The lateral boundaries are considered water tight too. The dimensions of each mesh have been chosen controlling the cleanness of the responses in frequency domain at an approximate free field control point. Details about the numerical validation of the used FE models by comparison with a substructure frequency-domain approach are provided below. As expected, the size of the required mesh grows with the mass of the superstructure. The DSSI FE meshes corresponding to C1L and C1M superstructures are shown in Fig.4.

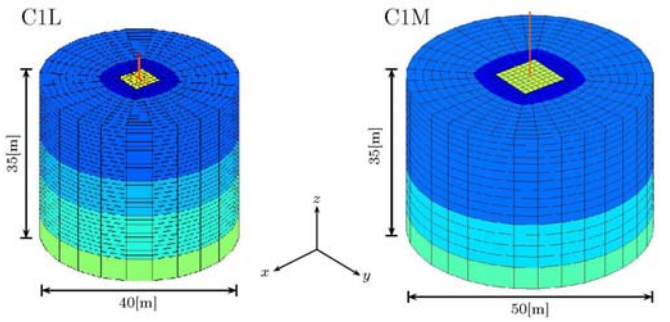

Fig. 4. Finite element meshes for SSI-N and SSI-E computations corresponding to C1L and C1M superstructures.

Colors displayed on meshes are related to different vertical dimension of elements. Darker colors close to the foundations correspond to a finer mesh zone used to compute some non-linear behavior indicators. It can be noticed that cylindrical geometries are used for the soil. Indeed, hydraulic boundary conditions at the corners of box-type meshes are delicate to model when the water table coincides with the free surface level in dynamics. In these corners, null normal flow must be ensured for lateral boundaries and free surface condition ($p=0$) has to be imposed at $z=0$ level. In order to avoid spurious flows under dynamical load, a suitable strategy is to eliminate corners using cylindrical meshes for the soil.

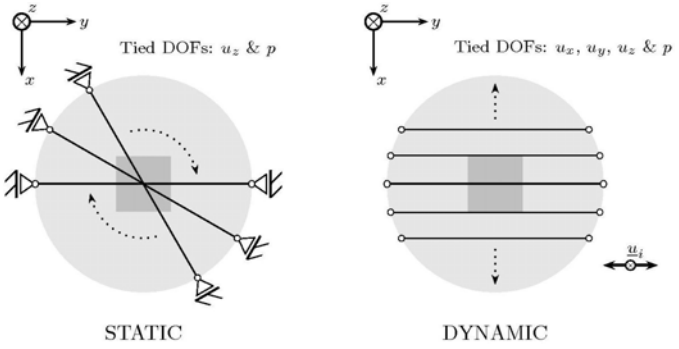

Fig. 5. Tied nodes approach for cylindrical meshes: static and dynamic cases.

For these cylindrical meshes, the tied nodes approach has been slightly adapted in both static and dynamic analyses. The static and dynamic configuration is shown in Fig.5. In the static part of the computation, we impose radial tied constraint as if the problem was axi-symmetric. Indeed, even if the problem is not perfectly axi-symmetrical in statics due to the square form of the foundation, we select lateral limits far enough to avoid border effects. In dynamic case, we impose tied nodes across the direction of the imposed shaking in order to impose shear-beam-like kinematics. We impose incident motions normal to one of the sides of square foundation for the sake of simplicity. Dynamic part of the analysis is conducted from the equilibrated state obtained in the static part of the analysis. Consequently, displacements, deformations, velocities and accelerations field correspond to a dynamic perturbation field around the static equilibrium.

Strong motion selection

The adopted strategy is based on the methodology proposed by Douglas (2006) in the framework of the VEDA (Seismic Vulnerability of structures: a Damage mechanics Approach) research project in which a part of this work was done. At present there are many sources of earthquake strong-motion records that could provide thousands of records as input to the structural models (e.g., Seekins *et al.*, 1992; Ambraseys *et al.*, 2004) or other Internet databases. However, as the studied FE models are complex and consequently take time to run, it is important that a small selection of strong-motion records be chosen in order to cut down the number of runs required but allowing to obtain general tendencies. In order to select an efficient set of input accelerograms some ideas from the theory of Design of Experiments (DOE) are employed.

The geographical scope of this study is France. In view of this, the database of strong-motion records developed by Ambraseys *et al.* (2004) has been chosen as the source of data for this work since it provides a large set of data mainly from moderate (M_w<*6.5*) shallow (*h*<*30*[km]) earthquakes that occurred within Europe and the Middle East. We consider a two-level of factorial design for three factors (strong-motion parameters). This implies eight runs. Running the entire design more than once permits to obtain average values of the responses as well as some ideas about the dispersion.

An earthquake can be characterized by measures of its frequency content, duration and severity/intensity measures. It is generally accepted that pure amplitude measures as PGA are not ideal measures of the severity/intensity of earthquakes, as they do not contain any information about the duration and the frequency content of strong ground motion, especially for problems involving stiffness degradation (Koutsourelakis *et al.*, 2002). Consequently, using parameters of severity/intensity including duration and frequency content information to characterize earthquake ground motions could lead to an improved prediction of earthquake damage. According to this, we choose three strong-motion parameters: significant duration T_{SR} (Trifunac and Brady, 1975); Arias intensity *AI* (Arias, 1970) and the mean period T_m (Rathje *et al.*, 1998), associated to duration, energy and frequency content, respectively. Additionally, as site effects are explicitly included in the FE model, only records on rock or stiff soil ($V_{s,30}$>*400*[m/s]) were considered. The ranges of the low and high bins are chosen according to geographical scope of this work (Metropolitan France) and are shown in Table 1.

Table 1. Sample of Table

Parameter	Low bin range	High bin range
T_{SR}	≤*10*[s]	>*10*[s]
AI	≤*0.07*[m/s]	>*0.07*[m/s]
T_m	≤*0.5*[s]	>*0.5*[s]

An experiment is constituted by 2^3=*8* records (or runs). Each experiment was repeated four times (*3* earthquakes selection), thus a total of *24* runs were conducted for each SDOF on each soil model.

ELASTIC DSSI

In order to highlight the influence of the elastic DSSI on the elastic dynamic response of the studied SDOFs, this section presents some spectral ratio amplitudes computed for C1L and C1M superstructures on both, dry and saturated homogenous sandy soils. We use the convention depicted in Fig.6 to indicate spectral ratios between free field and bedrock (ff/bd) and between the top of the structure and free field (tp/ff). The free field (ff) and bedrock (bd) control points are placed as far as possible from the superstructure, depending on the corresponding FE mesh. Indeed, the curves presented below were used to control the cleanness of the free field responses obtained in order to define a suitable mesh with a reasonable degree of wave reflections on its lateral borders.

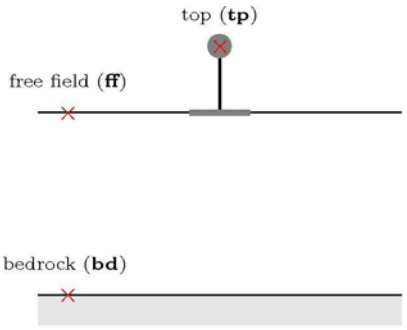

Fig. 6. Spectral ratio definitions.

Linear elastic DSSI numerical validation

In order to validate the numerical approach adopted in this paper, the problem will be treated by the substructure method in frequency domain using MISS3d code (Clouteau, 2000; Clouteau, 2003; Clouteau and Aubry, 2003), and by the direct method in time domain using *GEFDyn* FE software. As MISS3d code requires linear elasticity, we used linear elastic constitutive models for both soil and superstructure. We also impose that loss of contact between soil and foundation do not take place, thus we assume continuity of displacement and stress over the soil-structure interface.

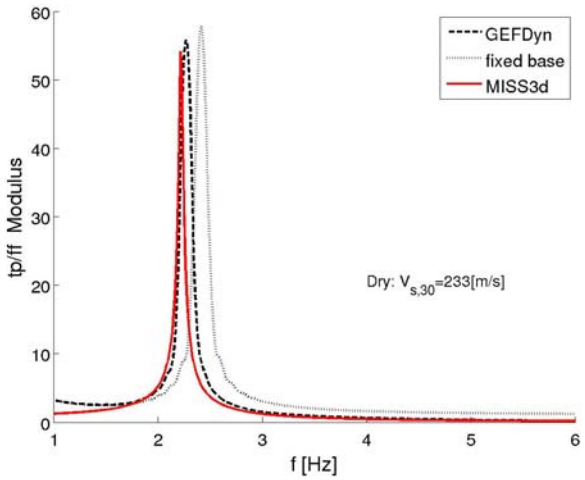

Fig. 7. Comparison between computed spectral ratio tp/ff modulus obtained with substructure and direct method: C1L on dry soil.

In substructure approach, the unbounded soil subdomain is modeled with BEM and its response is disjointed from the solution of the superstructural subdomain. The superstructure is a FE model identical to the used for the direct approach. The surface meshes required for the boundary of the soil over the soil-structure interface is deduced from the finite element mesh of the superstructure. The coupling between FEM and BEM is conducted using a modal reduction technique. We use the Craig-Bampton reduction technique to export the FE superstructure model to MISS3d code accounting the six rigid body modes (3 translations and 3 rotations) and the first fixed base mode. Concerning the damping, we use two different values: the first one is related to the superstructure and the second one is assumed for the soil and the bedrock. The superstructure damping ratio is used to construct a damping matrix as a linear combination of stiffness and mass matrix following traditional Rayleigh method. The damping representing the hysteretic soil energy dissipation, is introduced into equations using the correspondence principle in frequency domain on the soil and bedrock.

Fig.7 shows the comparison between the spectral ratio tp/ff obtained for both computations on dry soil and the transfer function of the C1L fixed base model. The agreement between both computations is excellent in frequency and modulus. A small shift of the main frequency is found and some reduction of amplitude can be noticed. The shift of the main frequency of the superstructure from *2.5*[Hz] to *2.25*[Hz] results from the flexibility of the foundation soil, whereas the change in the amplitude results from the material soil and radiation damping added. The numerical value of period shifting is compatible with the standard simple expression to compute linear-elastic soil-structure interaction. Similar agreement is found for C1L in saturated soil, and for C1M in both dry and saturated cases.

Free field responses

The obtained spectral ratio modulus between a free field control point and its vertical projection on the bedrock (ff/bd) are displayed in Fig.8.

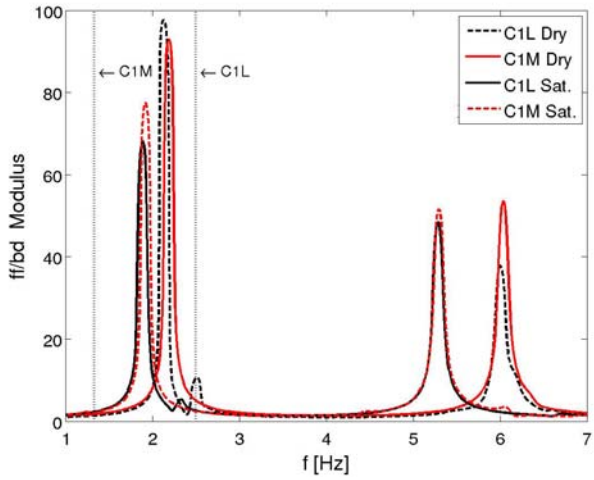

Fig. 8. Elastic spectral ratio modulus between free field and vertical projection on bedrock.

In dry soil condition, some evidences of the superstructure is found at the free field for the C1L structure. No perturbation appears for the C1M superstructure. This result is related to

the relative position of the fixed base fundamental frequency of the superstructure compared to the elastic frequencies of the soil profile. In C1L case, its fundamental frequency is relatively close to first elastic period of the soil, thus some resonance between both systems takes place. On the contrary, the first fixed base frequency of the C1M structure is relatively far from the first elastic frequency of the soil profile. Similarly, in the saturated soil case, some perturbations around the fundamental fixed base frequency of the C1L superstructure are found. No effect of the C1M structure is noticed.

Differences between spectral ratio amplitudes computed for dry and saturated case are associated to the reduction of effective stresses due to the presence of pore water. Some small frequency shifts of the first elastic mode as well as amplitude variations can be noticed depending on the superstructure considered. This shift might be related to local confinement variation below the superstructure foundation. However, as meshes used for each structure are not identical, these variations could be also associated to wave dispersion and reflections. Additionally, as computations are carried out in time domain, spectral ratio computations in frequency domain involve interpolations, filtering and smoothing procedures. These numerical procedures could also induce some shift in main frequencies and variation of amplitudes.

SOIL RESPONSE

In order to define the input motion for TS-E and TS-N approaches, the wave propagation part of the problem is solved using a 1D FE column. Fig.9 shows the responses for both soils in terms of the amplitude of the acceleration at free field (*PGA*) and the amplitude of the acceleration imposed at outcrop (a_{out}) for the 24 motions considered.

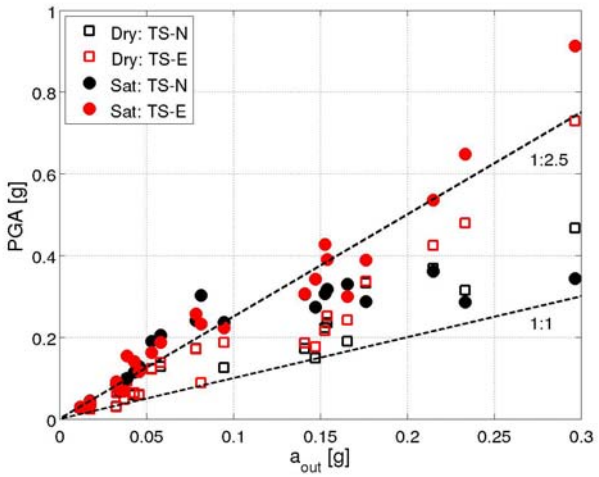

Fig. 9. Computed PGA as a function of the acceleration amplitude imposed at outcropping bedrock a_{out}.

If the elastoplastic behavior of the soil is taken into account (TS-N), the amplification of the soil deposit decays with the motion severity. Consequently, for strong motions, large accelerations are obtained when the elastic model (TS-E) is used. At low amplitude, as the response is essentially elastic, responses computed using both models are equivalent. The limit between elastic and non-linear behavior depends on the soil. For dry case, motions having an a_{out} large than *0.1g* induce non-linearities that attenuate the amplification. This limit is reduced when the soil is saturated. In this last case, for a_{out} larger than *0.03g* the non-linear behavior takes place. The variation in this limit is related to the initial stiffness of the soil. Assuming that a similar shear stress is imposed by an earthquake independently of the soil properties, smaller strains are obtained for stiffer soils. Consequently, the saturated soil undergoes larger shear strain producing more hysteretic behavior for small levels of imposed shear stress compared to dry case. Differences between elastic and inelastic soil acceleration amplification grow in general with the amplitude. In dry case, relatively small variations are obtained for $a_{out}<0.2g$. For larger outcrop amplitudes, significant differences are noticed between two behaviors. In saturated case, large differences start at *0.15g*. In this last hydraulic condition, there are moderate motions ($0.05g<a_{out}<0.1g$) exhibiting larger amplification in the inelastic case compared to the elastic one. This behavior might be related to the frequency content of the motion relative to inelastic transfer function of the soil profile during the motion. Indeed, the pore pressure build-up during the earthquake can acts as a frequency filter modifying significantly the frequency characteristic of the obtained motion at free field. When an elastic behavior model is considered, shear strains do not induce volumetric strains. Consequently, pore pressure build up does not take place and the filter effect vanishes.

EFFECT OF DSSI ON THE SEISMIC DISPLACEMENT DEMAND

In order to study the influence of the elastic and inelastic DSSI on the superstructure, this section presents computed displacement demand for different combinations of soil, superstructure and soil constitutive models according to two-step and full 3D approaches described above. Results are presented in the form of scatter plots of the computed ductility ratio demand μ defined as:

$$\mu = \frac{1}{D_y} \max_t \left\{ u^{top}(t) - u^{base}(t) - h.\theta(t) \right\} \quad (3)$$

where $u^{top}(t)$ and $u^{base}(t)$ are the nodal displacement time histories computed at the top and at the base of the SDOF in the direction of the seismic loading, respectively. $\theta(t)$ is the rigid body rotation (tilt) time history of the superstructure in full 3D models and h is its height. D_y is the corresponding yield displacement shown in Fig.2. If the obtained value of μ is less than *1*, the structure behaves elastically and a value of $\mu=1$ is imposed. For two-step computations, the base displacement u^{base} and the rigid body rotation θ are equal to zero, thus the ductility ratio is directly computed with the maximum top displacement and D_y.

In order to use a common reference for different type of computations, we use motion's severity measures at outcropping. Nevertheless, the effective motion transmitted to superstructure varies in each case due to local soil condition and DSSI effects. As discussed previously, measures of energy of the input motion show better correlation with the dynamic responses than pure amplitude measures. Consequently, we use Arias intensities at outcropping AI_{out} hereinafter. Concerning the used strong motion database, unrealistic displacement demands were obtained for one of the selected records. Even if this motion has been reported as recorded on very stiff soil, an approximately two-times larger AI_{out} is associated to this motion compared to other records in the selection, suggesting some site effects. As results of these observations, we decide to remove this motion from the set of results.

In order to summarize the effect of taking into account or neglecting inelastic soil behavior on the seismic demand, we compute the ratio:

$$\Delta\mu = \frac{\mu_{SSI} - \mu_{TS}}{\mu_{TS}} \quad (4)$$

where μ_{SSI} and μ_{TS} are the displacement ductility demands obtained from SSI-N or SSI-E and TS-N or TS-E, respectively. A positive value of $\Delta\mu$ means detrimental DSSI effect, and the opposite when the value is negative.

C1L SDOF on dry soil

Fig.10 shows the obtained ductility ratios for the C1L SDOF on dry soil, for both elastic and inelastic soil constitutive models. In both cases, for weak to moderate motions ($0.03<AI_{out}<0.15$), variations are erratic, so that depending on the motion, DSSI has a favorable or a detrimental effect on the computed ductility ratios. Clearer differences between two-step and full DSSI computations appear for motions having $AI_{out}>0.15$. In this range, DSSI has, in general, a detrimental effect independently of the constitutive model used for the soil. Only one strong motion shows favorable DSSI effects.

The increase of μ for severe motions is in opposite to the standard observations regarding DSSI effects. This unexpected behavior might be related to the modification of the properties of the local soil below the foundation and the relative position of the fundamental frequencies of the superstructure and the soil compared to the frequency content of the motions.

Concerning the soil behavior, assuming elastic or inelastic soil does not modify the general effect of the DSSI. Hence, motions exhibiting positive values for elastic soil, are also positive for inelastic soil. For this SDOF on dry soil, variations are inferior to ±25% for the major part of motions. According to our computations, results for C1L structure on dry soil are extremely erratic, consequently, more motions should be analyzed before any general tendencies could be derived. Examination of the results in terms of frequency content measures does not exhibit better tendencies.

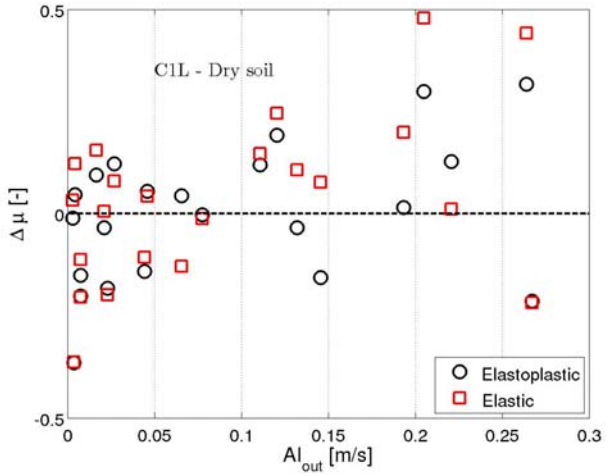

Fig. 10. Scatter plots of $\Delta\mu$ for the C1L SDOF on dry soil.

C1L SDOF on saturated soil

Results in terms of the computed ductility ratio following SSI-N/TS-N and SSI-E/TS-E approaches for the saturated soil are shown in Fig.11. Similar tendency as the one observed in dry case can be noticed for very weak motions ($AI_{out}<0.03$[m/s]), thus a reduction of the computed ductility demand ratio in the major part of cases. As concerns the range $0.03<AI_{out}<0.15$[m/s], the responses are erratic, hence depending on the motion an increase or a reduction in ductility demand is observed. For moderate to severe motion ($AI_{out}>0.15$[m/s]) different conclusions can be derived depending on the assumption taken for the soil behavior. In the inelastic soil case, all the considered cases show a reduction on the ductility demand when DSSI effects are taken into account. Under elastic soil assumption, this reduction is only noticed for two motions in this range. In fact, when the soil is modeled as a two-phase media and the inelastic soil's skeleton deformations are taken into account, volumetric deformations take place under dynamic loading. When the soil is assumed to behave elastically, pure shear strains do not induce volumetric variations and consequently the pore pressure build up does not take place. This pore pressure evolution contributes hardly to soil stiffness degradation and to hysteric soil damping. Consequently, the elastic soil behavior assumption is a crude hypothesis for the two-phase case. Thus, in saturated soil case, pure elastic DSSI considerations cannot explain differences found for ductility demands when the inelastic soil behavior is taken into account in the DSSI problem.

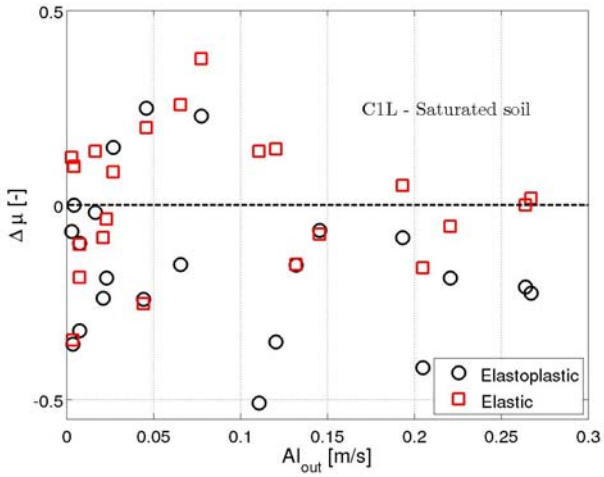

Fig. 11. Scatter plots of $\Delta\mu$ for the C1L SDOF on saturated soil.

C1M SDOF on dry soil

As concerns mid-rise SDOF (C1M), obtained $\Delta\mu$ for dry soil case are shown in Fig.12. The inelastic structural behavior is developed for motions having a severity $AI_{out}>0.03$[m/s] approximately. Only one motion with $AI_{out}=0.11$[m/s] does not show structural damage despite its severity. Indeed, this motion has a mean period T_m of *0.23*[s], hence the major part of the energy is delivered in a spectral range relatively far from the fundamental period of the superstructure ($T_0=0.75$[s]).

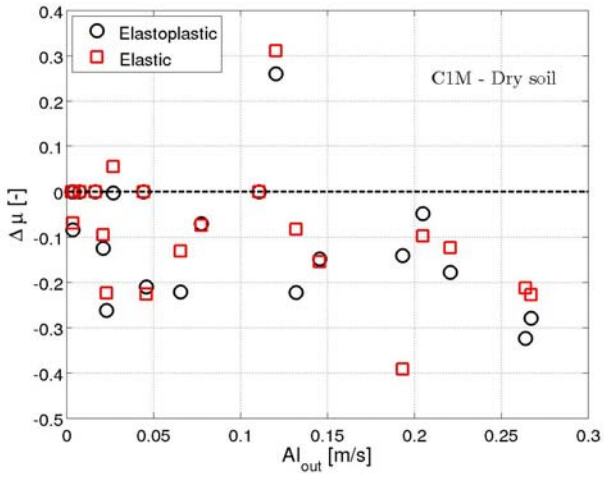

Fig. 12. Scatter plots of $\Delta\mu$ for the C1M SDOF on dry soil.

Regarding the effects of the DSSI on the superstructure response, the results depicted in Fig.12 agree with the standard DSSI effects, thus a general reduction of the seismic demand when DSSI are included. In contrast with responses obtained for C1L SDOF in dry soil (Fig.10), only one motion exhibits a clear detrimental effect of DSSI. As the mean period of this motion ($T_m=0.53$[s]) is relatively close to the first elastic period of the soil (*0.46*[s]), some resonance phenomena between soil and input motion might explain these differences.

On the basis of the responses displayed in Fig.10 and Fig.12, the inelastic soil behavior has a negligible effect on the superstructure's dynamic response when the soil is in dry condition. Indeed, the effect of the DSSI on the computed ductility demand is similar if the soil is assumed to behave elastically or inelastically regardless of the soil behavior. Consequently, for this soil and in the range of motion severities studied in this paper, an elastic DSSI analysis seems to be accurate enough to take into account interaction effects. Moreover, the effect of neglecting DSSI can be conservative or may not depend on the considered motion as noticed for C1L SDOF structure. As C1M is more slender and massive than C1L, larger dynamic soil-structure interaction effects seem to take place due to the superstructure rocking.

C1M SDOF on saturated soil

Concerning C1M SDOF structure on saturated soil, Fig.13 shows the variation of the seismic ductility demand ratios computed following SSI-N/TS-N and SSI-E/TS-E approaches. Similarly to responses obtained for C1L structure on saturated soil, when inelastic soil behavior is taken into account DSSI is benefic, thus a negative value of $\Delta\mu$ is noticed for almost all the considered motions. When the soil is assumed to behave elastically, the effect of DSSI can be beneficial or detrimental depending on the motion characteristics. Consequently, in contrast with the tendency observed for dry soil, elastic soil behavior assumption is a crude approximation to asses DSSI effects in saturated case. As previously indicated for elastic soil cases, no coupling between shear and volumetric strains is obtained for pure cyclic shear loading. Hence, variations on pore pressure during dynamic loading are neglected. In practice, depending on the soil contraction/dilation characteristics, strong pore pressure build-up might take places inducing large reductions in soil effective stresses which can result in soil stiffness degradation.

Similarly to the C1L SDOF structure case, elastic DSSI considerations are reasonably accurate for the C1M on dry soil, but are not suitable when the soil is in saturated condition. According to Fig.12 and Fig.13, DSSI is in general favorable or negligible when the inelastic soil behavior is taken into account. This tendency is not necessarily adequately predicted under elastic soil considerations. Additionally, large differences are found in the computed $\Delta\mu$ for the major part of motions, even if the detrimental/favorable tendency is correctly predicted by the elastic soil approach.

For both C1L and C1M structures on dry soil, it can be noticed that variations appear between elastic and inelastic soil computations. In other words, points do not coincide in

previous scatter plots of $\Delta\mu$ for several motions. Thus, radiation damping and soil flexibility associated to elastic DSSI cannot explain completely differences observed on the computed structural responses. However, as the effective motion transmitted to the structure is not exactly the same in both elastic and inelastic soil cases, part of this difference could be related to the non-linear behavior of the superstructure.

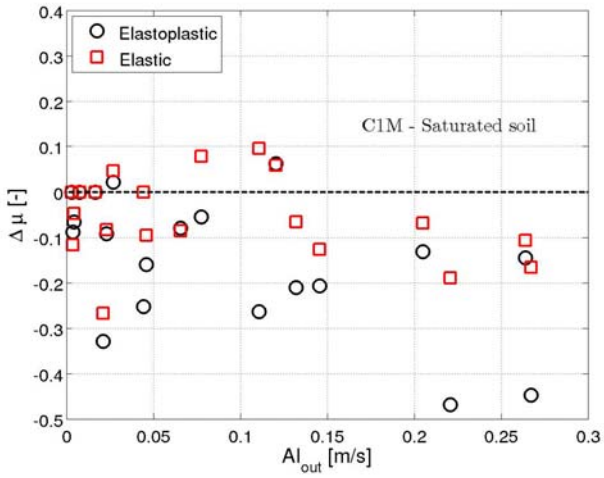

Fig. 13. Scatter plots of $\Delta\mu$ for the C1M SDOF on saturated soil.

In summary, the inelastic soil behavior seem to be not important for the structural dynamic response of C1L SDOF in dry soil. In this case, a traditional elastic DSSI analysis seems to be accurate enough to take into account interaction effects. For C1M SDOF on dry soil, some significant variation in structural damage are found when the soil behaves inelastically, and consequently, an inelastic soil behavior evaluation is desirable for this structure in this soil. For both superstructures, large variations of $\Delta\mu$ are found when the soil is saturated. Thus, a more precise assessment of the soil behavior might alters significantly the DSSI contribution evaluation to superstructure dynamic response.

CONCLUSIONS

This paper was devoted to identify the contribution of the inelastic soil behavior to the general non-linear DSSI problem. With this purpose, a comparative analysis between elastic and inelastic soil behavior assumptions was presented. In order to make as general as possible our results, we selected two generic SDOF structures taking values suggested in some seismic provisions. As the general problem of a shallow rigid foundation with SDOF structure is essentially three-dimensional, we used 3D FE models to analyze this problem. A homogenous medium dense sand soil profile in two hydraulic conditions (dry and saturated) has been used.

The results point out that, in general, inelastic soil behavior plays a decisive role only when the soil is saturated. When the soil is in dry condition, an elastic DSSI approach seems to be accurate enough to take into account the modification of the structural response due to dynamic interaction effects. Nevertheless, when the soil is saturated, large variations between elastic and inelastic DSSI approaches are found. As noted, these differences are related to pore pressure generation induced in the inelastic case which is neglected when elastic soil behavior is assumed.

Concerning the role of the DSSI on the dynamic response of both studied superstructures, the influence of interaction phenomena for the low-rise SDOF structure is quite erratic. Hence, depending on the characteristics of the ground motion DSSI effects are beneficial or detrimental in dry soil case. In saturated case, inelastic DSSI effects are in general beneficial. Regarding the mid-rise superstructure, in both dry and saturated soil cases, the effects of the DSSI are favorable in reducing the expected structural damage. These differences are probably due to the slenderness and mass of the mid-rise structure. Hence, larger interaction effects take place due to the rotation component of this slender superstructure.

Consequently, we can conclude that for the studied superstructures in dry soil, the DSSI phenomenon is mainly controlled by elastic effects, where the frequency content of the motion with respect to the elastic frequencies of the soil and the structure seem to define the role of the DSSI on the dynamic response of the structure system. Only in saturated case an influence of inelastic soil behavior is clear.

ACKNOWLEDGEMENTS

This work has benefited of a grant from the French "Agence National de la Recherche" in the framework of the VEDA (Seismic Vulnerability of structures: a Damage mechanics Approach) research project (ANR-05-CATT-017-01). First author has been financed partially by CONICYT-Embassy of France in Chile Postgraduate Fellowship Program and partially by BRGM.

REFERENCES

Ambraseys, N.N., Douglas, J., Sigbjörnsson, R., Berge-Thierry, C., Suhadolc, P., Costa, G. and Smit, P.M. [2004], *"Dissemination of European Strong- Motion Data, vol. 2, using Strong-Motion Datascape Navigator"*, Engineering and Physical Sciences Research Council, CD-ROM collection.

Arias, A. [1970], "A measure of earthquake intensity", in *Seismic design for nuclear power plants*, MIT Press. Cambridge, Mass.

Aubry, D., Hujeux, J.C., Lassoudière, F. and Meimon, Y. [1982], "A double memory model with multiple mechanisms for cyclic soil behaviour", *Int. Symp. Num. Mod. Geomech.*, Balkena.

Aubry, D., Chouvet, D., Modaressi, A. and Modaressi, H. [1986], *"GEFDyn : Logiciel d'Analyse de Comportement Mécanique des Sols par Eléments Finis avec Prise en Compte du Couplage Sol-Eau-Air"*, Manuel Scientifique, LMSSMat, Ecole Centrale Paris, France.

Aubry, D. and Modaressi, A. [1996], *"GEFDyn: Manuel Scientifque"*, LMSSMat, Ecole Centrale Paris, France.

Avilés, J. and Pérez-Rocha, L.E. [1996], *"Evaluation of interaction effects on the system period and the system damping due to foundation embedment and layer depth"*, Soil Dynamics and Earthquake Engineering, No. 15, pp. 11-21.

Avilés, J. and Pérez-Rocha, L.E. [2003], *"Soil-structure interaction in yieding systems"*, Earthquake Engineering and Structrual Dynamics, No. 32, pp. 1749-1771.

Ciampoli, M. and Pinto, P. [1995], "Effects of soil-structure interaction on inelastic seismic response of bridge piers", Journal of Structural Engineering ASCE, No. 121, pp. 806-814.

Clouteau, D. [2000], *"ProMiss 0.2: Manuel Scientifique"*, LMSSMat, Ecole Centrale Paris, France.

Clouteau, D. [2003], *"Miss 6.3: Manuel Utilisateur"*, LMSSMat, Ecole Centrale Paris, France.

Clouteau, D. and Aubry, D. [2003], "Computational Soil-Structure Interaction", in *Boundary Element Methods for Soil-Structure Interaction*, Kluwer Academic Publishers, pp. 61-126.

Douglas, J. [2006], *"Selection of strong-motion records for use as input to the structural models of VEDA"*, Report BRGM/RP-54584-FR, BRGM, France.

Ghannad, M.A. and Jahankhah, H. [2007], *"Site-dependent strength reduction factors for soil-structure systems"*, Soil Dynamics and Earthquake Engineering, No. 27, pp. 99-110.

Gazetas, G. and Mylonakis, G. [2001], "Soil-structure interaction effects on elastic and inelastic structures", *Fourth International Conference on Recent Advances in Geotechnical Earthquake Engineering and Soil Dynamics. Symposium in Honor of Professor W.D. Liam Finn*, San Diego, California.

HAZUS-MH MR3 [2003], *"Multi-hazard Loss Estimation Methodology. Technical Manual"*, Federal Emergency Management Agency.

Hujeux, J.C. [1985], "Une loi de comportement pour le chargement cyclique des sols", in *Génie Parasismique*, Presse ENPC, pp. 287-302.

Jennings, P.C. and Bielak, J. [1973], *"Dynamics of building-soil interaction"*, Bulletin of the Seismological Society of America, No. 63, pp. 9-48.

Koutsourelakis, S., Prévost, J.H. and Deodatis, G. [2002], *"Risk assessment of an interacting structure-soil system due to liquefaction"*, Earthquake Engineering and Structural Dynamics, No. 31, pp. 851-879.

Lopez-Caballero, F., Modaressi, A. and Modaressi, H. [2007], *"Nonlinear numerical method for earthquake site response analysis I- elastoplastic cyclic model & parameter identification strategy"*, Bulletin of Earthquake Engineering, No. 5, pp. 303-323.

Luco, J.E. [1980], "Soil-structure interaction and identification of structural models", *Proc. of the ASCE Specially Conference in Civil Engineering and Nuclear Power*, Tennessee.

Modaressi H. and Benzenati, I. [1994], *"Paraxial approximation for poroelastic media"*, Soil dynamics and Earthquake Engineering, No. 13, pp. 117-129.

Priestley, N. and Parck, R. [1987], *"Strength and ductility of concrete bridges columns under seismic loading"*, ACI Structural Journal, No. 84, pp. 61-76.

Rathje, E.M., Abrahamson, N.A. and Bray, J.D. [1998], *"Simplified frequency content estimates of earthquake ground motions"*, Journal of Geotechnical and Geoenvironmental Engineering ASCE, No. 124, pp. 150-159.

Rodriguez, M. and Montes, R. [2000], "Seismic response and damage analysis of building supported on flexible soils", Earthquake Engineering and Structural Dynamics, No. 29, pp. 647-665.

Sáez, E., Lopez-Caballero, F. and Modaressi-Farahmand-Razavi, A. [2008], *"Effects of non-linear soil behaviour on the seismic performance evaluation of structures"*, Italian Geotechnical Journal, No. 2, pp. 63-76.

Sáez, E. [2009], *"Dynamic nonlinear soil-structure interaction"*, Ph.D. Thesis, Ecole Centrale Paris, France.

Sáez, E., Lopez-Caballero, F. and Modaressi-Farahmand-Razavi, A. [2009], "An energetic approach to take into account the effect of the seismic non-linear SSI on the performance-base design", *Proc. of the Int. Conf. on Performance-Based Design in Earthquake Geotechnical Engineering (IS-Tokyo 2009)*, Tokyo, Japan.

Schnabel, P.B., Lysmer, J. and Seed, H.B. [1972], *"SHAKE: a computer program for earthquake response analysis of horizontally layered sites"*, University of California, Berkeley, CA.

Seekins, L.C., Brady, A.G., Carpenter, C. and Brown, N. [1992], *"Digitized strong-motion accelerograms of North and Central American earthquakes 1933-1986"*, Digital Data Series DDS-7, CD-ROM.

Trifunac, M.D. and Brady, A.G. [1975], *"A study on the duration of strong earthquake ground motion"*, Bulletin of the Seismological Society of America, No. 65, pp. 581-626.

Veletsos, A.S. [1977], *"Dynamic of structure-foundation systems"* in Structural and Geotechnical Mechanics, Prentice Hall, Englewood Cliffs, New Jersey.

Veletsos, A.S. and Meek, A. [1974], *"Dynamic behavior of building-foundation systems"*, Earthquake Engineering and Structural Mechanics, No. 3, pp. 121-138.

Veletsos, A.S. and Nair, V.D. [1975], *"Seismic interaction of structures on hysteretic foundations"*, Journal of the Structural Division (ASCE), No. 101, pp. 109-129.

Wolf, J.P. [1985], *"Dynamic Soil-Structure Interaction"*, Prentice Hall, Englewood Cliffs, New Jersey.

Zienkiewicz, O.C. and Shiomi, T. [1984], *"Dynamic behaviour of saturated porous media: The generalized Biot formulation and its numerical solution"*, International Journal of Numerical and Analytical Methods of Geomechanics, No. 8, pp. 71-96.

Zienkiewicz, O.C., Bicanic, N. and Shen, F.Q. [1988], Earthquake input definition and the transmitting boundary conditions", in *Advances in Computational Nonlinear Mechanics*, Springer-Verlag, pp. 109-138.